DOI: https://doi.org/10.15407/pmach2026.01.006

UDC 539.3

LINEAR VIBRATIONS OF NANOTUBE-REINFORCED COMPOSITE CONICAL SHELL WITH RING STIFFENER

[1] Kostiantyn V. Avramov
kvavramov@gmail.com, ORCID: 0000-0002-8740-693X

[1] Borys V. Uspenskyi
Uspensky.kubes@gmail.com, ORCID: 0000-0001-6360-7430

[2] Borys H. Liubarskyi, ORCID: 0000-0002-2985-7345

[2] Oleksii A. Smetskykh, ORCID: 0009-0005-0238-9712

[1] Iryna V. Biblik, ORCID: 0000-0002-8650-1134

[1] Anatolii Pidhornyi Institute of Power Machines and Systems of NAS of Ukraine,
2/10, Komunalnykiv str., Kharkiv, 61046, Ukraine

[2] National Technical University "Kharkiv Polytechnic Institute", 2, Kyrpychova str., Kharkiv, 61002, Ukraine

Linear vibrations of thin-walled structure, which consists of nanotube-reinforced conical shell and ring stiffeners, are analyzed. Ring is attached at the end of truncated conical shell. Such shell structure describes adapter of rocket. Dynamic of such structure is actual problem of aerospace engineering. Material of this shell is nanocomposite, and ring is manufactured from isotropic material. Higher order shear deformation theory for the shell and Euler-Bernoulli theory for ring stiffeners are applied. The Rayleigh-Ritz method is used to derive the equations of the structure vibrations. The potential energy of the thin-walled structure is used. This potential energy consists of potential energy of the conical shell and potential energy of the ring. It is assumed that the ring vibrates in two perpendicular planes, performs vibrations in circumference directions, and torsional vibrations occur. The least action variational principle is used. As a result, the generalized eigenvalue problem is derived. The data of eigenfrequencies calculations is verified by finite element calculations in ANSYS software.

***Keywords**: functionally graded carbon nanotube-reinforced composite, truncated conical shell, parameters of linear vibrations.*

Introduction

Nanotubes have much higher mechanical properties than steel and carbon fiber [1]. For example, the elastic modulus of nanotube is 100 times greater than one of steel. Therefore, the nanotubes are used to reinforce the composite. The obtained nanocomposite is light and strong. Therefore, these nanocomposites are used in aeronautic engineering.

Numerical analysis of mechanical properties of nanocomposites is very important for structures design. Liu and Chen [2] apply finite element technique to calculate reinforced nanotube composite mechanical characteristics. Odegard with coauthors [3] propose atomic model of nanocomposite.

Several efforts were made to experimentally analyze nanocomposite properties. Allaoui and coauthors [4] analyze nanocomposite tension. Ci and Bai [5] experimentally study influence of nanotubes distributions on nanocomposite characteristics. As follows from the experimental data [6], the nanocomposite ultimate strength is increased if number of nanotubes is increased. Nejati with coauthors [7] use rule of mixture to predict nanocomposite properties, which are obtained experimentally.

Linear nanocomposite shell mathematical models are derived to analyze static and dynamic structures response in [8, 9]. Nanocomposite plate vibrations are considered in several papers [10–12]. Impact dynamics of nanocomposite cylindrical shell is analyzed in [13].

Free linear vibrations of the conical shell with ring reinforcement are studied numerically in this paper. Nanotube reinforced functionally graded composite is used for shell. Euler-Bernoulli model is implemented for isotropic ring modeling. Rayleigh-Ritz method is used to study thin-walled structure vibrations. The obtained eigenfrequencies are compared with ones that are calculated in ANSYS software.

Model of thin-walled structure

Nanotube reinforced conical shell with ring from isotropic material is studied. The conical shell is analyzed in coordinate system (x, φ, z), which is shown on Fig. 1, a. The sketch of the ring is presented on Fig. 1, b and the whole structure is shown on Fig. 1, c. The ring coordinate system is related to the cross section of the ring (x_1, z_1).

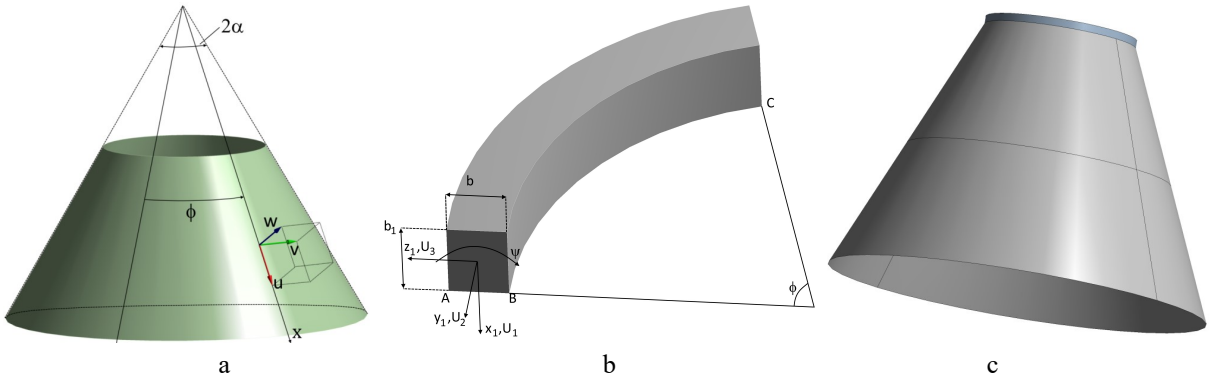

Fig. 1. Outline of joined structure

Nanotubes are aligned along *x* axis. Principal sketches of nanotubes reinforcements of shell are shown on Fig. 2. This figure shows five types of nanotube distributions in thickness direction *z*, namely: UD, FG-V, FG-Λ, FG-X, FG-O. The distribution functions of nanotubes in the thickness direction $V_{CNT}(z)$ for different types of nanotube reinforcements are shown in Table 1.

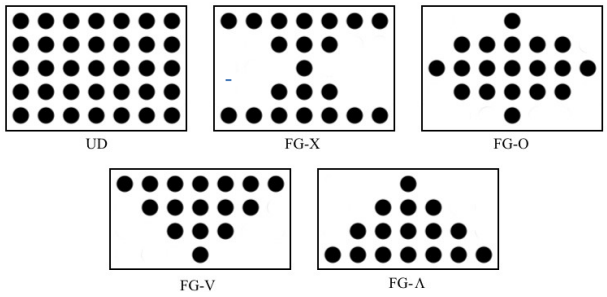

Fig. 2. Nanotube reinforcements of conical shell

Table 1. The dependences of nanotube distributions in the thickness directions

Reinforcements	Nanotube distributions
UD-CNT	$V_{CNT}(z)=V_{CNT}^{*}$
FGV-CNT	$V_{CNT}(z)=\left(1+\frac{2z}{h}\right)V_{CNT}^{*}$
FGΛ-CNT	$V_{CNT}(z)=\left(1-\frac{2z}{h}\right)V_{CNT}^{*}$
FGX-CNT	$V_{CNT}(z)=\frac{4\lvert z\rvert}{h}V_{CNT}^{*}$
FGO-CNT	$V_{CNT}(z)=2\left(1-\frac{2\lvert z\rvert}{h}\right)V_{CNT}^{*}$

The rule of mixture is used to obtain the mechanical characteristics of the material

$$E_{11}(z)=\eta_1 V_{CNT}(z)E_{11}^{CNT}+V_m(z)E^m;\quad E_{22}(z)=\frac{\eta_2 E_{22}^{CNT}E^m}{V_{CNT}(z)E^m+V_m(z)E_{22}^{CNT}};$$

$$G_{12}(z)=\frac{\eta_3 G_{12}^{CNT}G^m}{V_{CNT}(z)G^m+V_m(z)G_{12}^{CNT}};$$

$$\mu_{12}(z)=V_{CNT}(z)\mu_{12}^{CNT}+V_m(z)\mu^m;\quad \mu_{21}(z)=\frac{\mu_{12}(z)}{E_{11}(z)}E_{22}(z);$$

$$\rho(z)=V_{CNT}(z)\rho^{CNT}+V_m(z)\rho^m;\quad V_m(z)=1-V_{CNT}(z)$$

where indexes 1, 2, 3 are identical to *x*, φ, *z*; E_{11}^{CNT}, E_{22}^{CNT}, G_{12}^{CNT} are elastic and shear modules; η_1, η_2, η_3 are nanotube/matrix efficiency parameters; E^m, G^m are elastic and shear modulus of the matrix; ρ^{CNT}, ρ^m are densities of the nanotubes and the matrix. The Hooke's law of the considered composite is

$$\begin{bmatrix}\sigma_{11}\\ \sigma_{22}\end{bmatrix}=\begin{bmatrix}Q_{11}(z) & Q_{12}(z)\\ Q_{12}(z) & Q_{22}(z)\end{bmatrix}\cdot\begin{bmatrix}\varepsilon_{11}\\ \varepsilon_{22}\end{bmatrix};\quad \sigma_{13}=G_{13}(z)\gamma_{13};\quad \sigma_{12}=G_{12}(z)\gamma_{12},$$

where $Q_{11}(z)=\frac{E_{11}(z)}{1-\mu_{12}(z)\mu_{21}(z)}$; $Q_{22}(z)=\frac{E_{22}(z)}{1-\mu_{12}(z)\mu_{21}(z)}$; $Q_{12}(z)=\frac{\mu_{21}(z)E_{11}(z)}{1-\mu_{12}(z)\mu_{21}(z)}$.

The stressed state of the conical thin-walled structure is analyzed. The middle surface circle has the radius $r = x\sin\alpha$. The curvature radius of the middle surface is $R_\varphi = x\,\mathrm{tg}\alpha$. The shear and rotatory inertia are considered. The shear deformation theory [14] is applied. The displacement projections of the structure on the generating line and on the circumferential axes are denoted by u_x, u_φ. The displacement projections to the thickness direction are u_z. The structure displacements are the following

$$u_x = u(x,\varphi,t) + z\psi_x(x,\varphi,t) + z^2\theta_x + z^3\gamma_x;\ u_\varphi = \left(1+\frac{z}{R_\varphi}\right)v(x,\varphi,t) + z\psi_\varphi(x,\varphi,t) + z^2\theta_\varphi + z^3\gamma_\varphi;\ u_z = w(x,\varphi,t) \qquad (1)$$

where u, v, w are displacement projections of the middle surface; ψ_x, ψ_φ are rotation angles. The parameters θ_x, γ_x, θ_φ, γ_φ are derived from the boundary conditions: $\tau_{xz}\big|_{z=\pm 0.5h} = \tau_{\varphi z}\big|_{z=\pm 0.5h} = 0$; h is shell thickness;

$$\tau_{xz} = G_{13}(z)\left(\frac{\partial u_x}{\partial z} + \frac{\partial u_z}{\partial x}\right);\quad \tau_{\varphi z} = G_{23}(z)\left[\frac{\partial u_\varphi}{\partial z} + \frac{1}{1+zR_\varphi^{-1}}\left(\frac{\partial u_z}{r\partial\varphi} + \frac{u_\varphi}{R_\varphi}\right)\right];$$

$$\theta_x = 0;\quad \gamma_x = -\frac{4}{3h^2}\left(\frac{\partial w}{\partial x} + \psi_x\right);\quad \theta_\varphi = \frac{1}{2R_\varphi r}\frac{\partial w}{\partial\varphi} + \frac{1}{2R_\varphi}\psi_\varphi;\quad \gamma_\varphi = -\frac{8R_\varphi^2 + h^2}{6R_\varphi^2 h^2}\psi_\varphi - \frac{\left(8R_\varphi^2 - h^2\right)}{6rh^2R_\varphi^2}\frac{\partial w}{\partial\varphi} - \frac{v}{3R_\varphi^3}.$$

The elements of the strains tensor meet the following equations [15]

$$\varepsilon_{xx} = \varepsilon_{x,0} + z\left(k_x^{(0)} + zk_x^{(1)} + z^2k_x^{(2)}\right);\quad \varepsilon_{\varphi\varphi} = \varepsilon_{\varphi,0} + z\left(k_\varphi^{(0)} + zk_\varphi^{(1)} + z^2k_\varphi^{(2)}\right); \qquad (2)$$

$$\gamma_{x\varphi} = \gamma_{x\varphi,0} + z\left(k_{x\varphi}^{(0)} + zk_{x\varphi}^{(1)} + z^2k_{x\varphi}^{(2)}\right);\quad \gamma_{xz} = \gamma_{xz,0} + z\left(k_{xz}^{(0)} + zk_{xz}^{(1)} + z^2k_{xz}^{(2)}\right);\quad \gamma_{\varphi z} = \gamma_{\varphi z,0} + z\left(k_{\varphi z}^{(0)} + zk_{\varphi z}^{(1)} + z^2k_{\varphi z}^{(2)}\right).$$

The summands of the expansion (2) are obtained by Maple software. Therefore, the expressions for the summands of the expansion (2) are not given in this paper.

The strain energy of the conical shell is the following

$$\Pi = 0.5\iiint_V \left\{Q_{11}(z)\varepsilon_{xx}^2 + 2Q_{12}(z)\varepsilon_{\varphi\varphi}\varepsilon_{xx} + Q_{22}(z)\varepsilon_{\varphi\varphi}^2 + G_{23}(z)\gamma_{\varphi z}^2 + G_{13}(z)\gamma_{xz}^2 + G_{21}(z)\gamma_{x\varphi}^2\right\}\left(1+\frac{z}{R_\varphi}\right)dz\,dx\,d\varphi, \quad (3)$$

where V is shell volume. The equations (2) are used in (3). The strains energy is the following

$$\Pi = 0.5\iint_A r\,dx\,d\varphi\sum_{j=0}^{5} h_j,$$

where A is middle surface of conical shell;

$$h_0 = \widetilde{P}_0^{(0)};\quad h_j = \widetilde{P}_j^{(j)} + \frac{\widetilde{P}_{j-1}^{(j)}}{R_\varphi};\ j=1,\ \ldots,\ 5;$$

$$\widetilde{P}_0^{(j)} = Q_{11}^{(j)}\varepsilon_{x,0}^2 + 2Q_{12}^{(j)}\varepsilon_{x,0}\varepsilon_{\varphi,0} + Q_{22}^{(j)}\varepsilon_{\varphi,0}^2 + G_{23}^{(j)}\gamma_{\varphi z,0}^2 + G_{13}^{(j)}\gamma_{xz,0}^2 + G_{21}^{(j)}\gamma_{x\varphi,0}^2;$$

$$\widetilde{P}_1^{(j)} = 2Q_{11}^{(j)}\varepsilon_{x,0}k_x^{(0)} + 2Q_{12}^{(j)}\left(\varepsilon_{x,0}k_\varphi^{(0)} + \varepsilon_{\varphi,0}k_x^{(0)}\right) + 2Q_{22}^{(j)}\varepsilon_{\varphi,0}k_\varphi^{(0)} + 2G_{21}^{(j)}\gamma_{x\varphi,0}k_{x\varphi}^{(0)};$$

$$\widetilde{P}_2^{(j)} = Q_{11}^{(j)}k_x^{(0)2} + 2Q_{12}^{(j)}\left(\varepsilon_{x,0}k_\varphi^{(1)} + k_\varphi^{(0)}k_x^{(0)}\right) + Q_{22}^{(j)}\left(k_\varphi^{(0)2} + 2\varepsilon_{\varphi,0}k_\varphi^{(1)}\right) + 3G_{23}^{(j)}\gamma_{\varphi z,0}k_{\varphi z}^{(1)} + 2G_{13}^{(j)}\gamma_{xz,0}k_{xz}^{(1)} + G_{21}^{(j)}\left(2\gamma_{x\varphi,0}k_{x\varphi}^{(1)} + k_{x\varphi}^{(0)2}\right);$$

$$\widetilde{P}_3^{(j)} = 2Q_{11}^{(j)}k_x^{(2)}\varepsilon_{x,0} + 2Q_{12}^{(j)}\left(\varepsilon_{x,0}k_\varphi^{(2)} + k_\varphi^{(1)}k_x^{(0)} + k_x^{(2)}\varepsilon_{\varphi,0}\right) + 2Q_{22}^{(j)}\left(k_\varphi^{(0)}k_\varphi^{(1)} + \varepsilon_{\varphi,0}k_\varphi^{(2)}\right) + 2G_{21}^{(j)}\left(\gamma_{x\varphi,0}k_{x\varphi}^{(2)} + k_{x\varphi}^{(0)}k_{x\varphi}^{(1)}\right);$$

$$\widetilde{P}_4^{(j)} = 2Q_{11}^{(j)}k_x^{(2)}k_x^{(0)} + 2Q_{12}^{(j)}\left(k_\varphi^{(2)}k_x^{(0)} + k_x^{(2)}k_\varphi^{(0)}\right) + Q_{22}^{(j)}\left(k_\varphi^{(0)2} + 2k_\varphi^{(2)}k_\varphi^{(0)}\right) + 2G_{13}^{(j)}k_{xz}^{(1)2} + G_{21}^{(j)}\left(k_{x\varphi}^{(1)2} + 2k_{x\varphi}^{(0)}k_{x\varphi}^{(2)}\right) + G_{23}^{(j)}k_{\varphi z}^{(1)2};$$

$$\widetilde{P}_5^{(j)} = 2Q_{12}^{(j)}k_\varphi^{(1)}k_x^{(2)} + 2Q_{22}^{(j)}k_\varphi^{(2)}k_\varphi^{(1)} + 2G_{21}^{(j)}k_{x\varphi}^{(1)}k_{x\varphi}^{(2)}.$$

The kinetic energy takes the form

$$T = 0.5\iiint_V \rho(z)\left(u_x^2 + u_\varphi^2 + u_z^2\right)\left(1+\frac{z}{R_\varphi}\right)dz\,r\,dx\,d\varphi, \qquad (4)$$

where $\dot{u}_x = \dfrac{\partial u_x}{\partial t}$. The expansion (1) is used in the kinetic energy (4). Then the kinetic energy is the following

$$T = 0.5\iint\limits_A r\,dx\,d\varphi \sum_{j=0}^{5} r_j P_j ,$$

where

$$r_j = \int\limits_{-0.5h}^{0.5h} z^j \rho(z)\,dz ; \quad j=0,\ 1,\ \ldots;\ P_0 = \dot{u}^2 + \dot{v}^2 + \dot{w}^2 ;$$

$$P_1 = 2\dot{u}\dot{\psi}_x + \frac{2\dot{v}^2}{R_\varphi} + 2\dot{v}\dot{\psi}_\varphi + \frac{1}{R_\varphi}\left(\dot{u}^2 + \dot{v}^2 + \dot{w}^2\right);$$

$$P_2 = \dot{\psi}_x^2 + \frac{\dot{v}^2}{R_\varphi^2} + \dot{\psi}_\varphi^2 + \frac{2}{R_\varphi}\dot{v}\dot{\psi}_\varphi + 2\dot{v}\dot{\theta}_\varphi + \frac{1}{R_\varphi}\left(2\dot{u}\dot{\psi}_x + \frac{2\dot{v}^2}{R_\varphi} + 2\dot{v}\dot{\psi}_\varphi\right);$$

$$P_3 = 2\dot{u}\dot{\gamma}_x + \frac{2}{R_\varphi}\dot{v}\dot{\theta}_\varphi + 2\dot{v}\dot{\gamma}_\varphi + 2\dot{\psi}_\varphi\dot{\theta}_\varphi + \frac{1}{R_\varphi}\left(\dot{\psi}_x^2 + \frac{\dot{v}^2}{R_\varphi^2} + \dot{\psi}_\varphi^2 + \frac{2}{R_\varphi}\dot{v}\dot{\psi}_\varphi + 2\dot{v}\dot{\theta}_\varphi\right);$$

$$P_4 = 2\dot{\psi}_x\dot{\gamma}_x + \dot{\theta}_\varphi^2 + \frac{2}{R_\varphi}\dot{v}\dot{\gamma}_\varphi + 2\dot{\psi}_\varphi\dot{\gamma}_\varphi + \frac{1}{R_\varphi}\left(2\dot{u}\dot{\gamma}_x + \frac{2}{R_\varphi}\dot{v}\dot{\theta}_\varphi + 2\dot{v}\dot{\gamma}_\varphi + 2\dot{\psi}_\varphi\dot{\theta}_\varphi\right);$$

$$P_5 = 2\dot{\theta}_\varphi\dot{\gamma}_\varphi + \frac{1}{R_\varphi}\left(2\dot{\psi}_x\dot{\gamma}_x + \dot{\theta}_\varphi^2 + \frac{2}{R_\varphi}\dot{v}\dot{\gamma}_\varphi + 2\dot{\psi}_\varphi\dot{\gamma}_\varphi\right).$$

The lower edge of thin-walled structure is clamped

$$u\big|_{x=L_2} = v\big|_{x=L_2} = w\big|_{x=L_2} = \psi_x\big|_{x=L_2} = \psi_\varphi\big|_{x=L_2} = 0 ,$$

where L_2 is cone generating line length.

The ring is attached to the upper edge of the structure $x=L_1$. This ring is very important for the launch vehicles adapters. The explosive bolts are attached to adapters in order to separate the launch vehicle. But it is very important to reduce the amplitudes of the adapters vibrations to preserve the electronic equipment in operable conditions. Therefore, the considered problem is very important for aeronautic engineering.

The deformations of the ring are modeled by Euler-Bernoulli theory [16]. The ring bending is described by two displacements – $\overline{u}(\varphi,t)$ and $\overline{w}(\varphi,t)$ – in two perpendicular planes. The ring compression/tension is modeled by $\overline{v}(\varphi,t)$. Moreover, the ring performs torsional vibrations $\psi(\varphi,t)$. Displacements of arbitrary points of beam U_1, U_2, U_3 satisfy the equations:

$$U_1 = \overline{u}(\varphi,t) - z_1\psi(\varphi,t) ; \quad U_2 = \overline{v}(\varphi,t) + x_1\psi_1(\varphi,t) - z_1\psi_2(\varphi,t) ; \quad U_3 = \overline{w}(\varphi,t) + x_1\psi(\varphi,t)$$

where $\psi_1(\varphi, t)$, $\psi_2(\varphi, t)$ are rotation angles of the ring cross section. The ring cross sections coordinates x_1, z_1 are shown on Fig. 1, b. The hoop strains take the form [16]

$$\varepsilon_{\varphi\varphi} = \varepsilon_\varphi - x_1\chi_X + z_1\chi_r ,$$

where χ_x and χ_r are curvature variation. The values ε_φ, χ_x, χ_r are calculated as [16]

$$\varepsilon_\varphi = \frac{1}{R_r}\frac{\partial\overline{v}}{\partial\varphi} + \frac{\overline{w}}{R_r} ; \quad \chi_x = \frac{1}{R_r^2}\frac{\partial^2\overline{u}}{\partial\varphi^2} - \frac{\overline{w}}{R_r} ; \quad \chi_r = -\frac{1}{R_r^2}\frac{\partial^2\overline{w}}{\partial\varphi^2} + \frac{1}{R_r^2}\frac{\partial\overline{v}}{\partial\varphi} ,$$

where R_r is ring radius. The shear strains of the ring $\gamma = \sqrt{x_1^2 + y_1^2}\,\chi(\varphi,t)$;

$$\chi(\varphi,t) = -\frac{1}{R_r}\frac{\partial\psi}{\partial\varphi} + \frac{\psi_1}{R_r} .$$

The ring strain energy is

$$\Pi_1 = 0.5\int_0^{2\pi}\left(EA\varepsilon_\varphi^2 + EJ_x\chi_x^2 + EJ_r\chi_r^2 + GJ\chi^2\right)R_r\, d\varphi,$$

where E, G are elastic and shear modulus; $J_x = \iint_{A_1} x_1^2 dx_1 dz_1$; $J_r = \iint_{A_1} z_1^2 dx_1 dz_1$; $J = \iint_{A_1}(x_1^2 + z_1^2)dx_1 dz_1$.

The matching conditions of joining of conical shell and ring take the form

$$\widetilde{U}_2 = v\big|_{x=L_1};\quad \widetilde{U}_3 = u\big|_{x=L_1}\sin\alpha + w\big|_{x=L_1}\cos\alpha;\ \widetilde{U}_1 = u\big|_{x=L_1}\cos\alpha - w\big|_{x=L_1}\sin\alpha,$$

where $\widetilde{U}_1 = U_1\big|_{z_1=0}$; $\widetilde{U}_2 = U_2\big|_{z_1=0;x_1=0.5b_1}$; $\widetilde{U}_3 = U_3\big|_{x_1=0.5b_1}$. The equality of rotating angles of ring and shell are [17]

$$\psi = -\psi_x(L_1,\varphi);\quad \psi_2 = -\psi_\varphi(L_1)\cos\alpha;\quad \psi_1 = -\psi_\varphi(L_1)\sin\alpha.$$

The ring displacements and the shell generalized displacements satisfy the equations

$$\begin{gathered}\overline{v}(\varphi,t) = v(L_1,\varphi,t) + 0.5b_1\psi_\varphi(L_1,\varphi,t)\sin\alpha;\\ \overline{w}(\varphi,t) = u(L_1,\varphi,t)\sin\alpha + w(L_1,\varphi,t)\cos\alpha + 0.5b_1\psi_x(L_1,\varphi,t);\\ \overline{u}(\varphi,t) = u(L_1,\varphi)\cos\alpha - w(L_1,\varphi)\sin\alpha.\end{gathered} \tag{5}$$

The parameters ε_φ, χ_x, χ_r, χ can be calculated as

$$\varepsilon_\varphi = \frac{1}{R_r}\left\{\frac{\partial v(L_1,\varphi)}{\partial\varphi} + 0.5b_1\sin\alpha\frac{\partial\psi_\varphi(L_1,\varphi)}{\partial\varphi} + w(L_1,\varphi)\cos\alpha + 0.5b_1\psi_x(L_1,\varphi) + u(L_1,\varphi)\sin\alpha\right\};$$

$$\chi_x = \frac{1}{R_r^2}\left(\frac{\partial^2 u(L_1,\varphi)}{\partial\varphi 2}\cos\alpha - \frac{\partial^2 w(L_1,\varphi)}{\partial\varphi^2}\sin\alpha\right) + \frac{\psi_x(L_1,\varphi)}{R_r};$$

$$\chi_r = \frac{1}{R_r^2}\left\{\frac{\partial v(L_1,\varphi)}{\partial\varphi} + 0.5b_1\frac{\partial\psi_\varphi(L_1,\varphi)}{\partial\varphi}\sin\alpha - \frac{\partial^2 w(L_1,\varphi)}{\partial\varphi^2}\cos\alpha - 0.5b_1\frac{\partial^2\psi_x(L_1,\varphi)}{\partial\varphi^2} - \frac{\partial^2 u(L_1,\varphi)}{\partial\varphi^2}\sin\alpha\right\};$$

$$\chi = \frac{1}{R_r}\frac{\partial\psi_x(L_1,\varphi)}{\partial\varphi} - \frac{\sin\alpha}{R_r}\psi_\varphi(L_1,\varphi).$$

The ring kinetic energy has the form

$$T_1 = 0.5\int_0^{2\pi} R_r d\varphi\iint_{A_1}\rho_r\left[\left(\frac{\partial U_1}{\partial t}\right)^2 + \left(\frac{\partial U_2}{\partial t}\right)^2 + \left(\frac{\partial U_3}{\partial t}\right)^2\right]dx_1\, dz_1,$$

where ρ_r is ring material density. The kinetic energy of the ring is the following

$$T_1 = 0.5\rho_r A\int_0^{2\pi}\left\{\left(\frac{\partial\overline{u}}{\partial t}\right)^2 + \left(\frac{\partial\overline{v}}{\partial t}\right)^2 + \left(\frac{\partial\overline{w}}{\partial t}\right)^2 + \frac{J}{A}\left(\frac{\partial\psi}{\partial t}\right)^2\right\}R_r\, d\varphi. \tag{6}$$

The ring kinetic energy is derived with respect to the conical shell displacements. The equations (5) are substituted into the kinetic energy (6)

$$T_1 = 0.5\rho_r A\int_0^{2\pi} R_r\, d\varphi\left\{\left(\frac{\partial u(L_1,t)}{\partial t}\cos\alpha - \frac{\partial w(L_1,\varphi,t)}{\partial t}\sin\alpha\right)^2 + \left(\frac{\partial u(L_1,\varphi,t)}{\partial t}\sin\alpha + \frac{\partial w(L_1,\varphi,t)}{\partial t}\cos\alpha + 0.5b_1\frac{\partial\psi_x(L_1,\varphi,t)}{\partial t}\right)^2 +$$

$$+\left(\frac{\partial v(L_1,\varphi,t)}{\partial t} + 0.5b_1\frac{\partial\psi_\varphi(L_1,\varphi,t)}{\partial t}\sin\alpha\right)^2 + \frac{J}{A}\left(\frac{\partial\psi_x(L_1,\varphi,t)}{\partial t}\right)^2\right\}.$$

The kinetic and potential energies of the whole structure T_Σ, Π_Σ are

$$T_\Sigma = T + T_1;\quad \Pi_\Sigma = \Pi + \Pi_1.$$

Linear vibrations of structure

The Rayleigh-Ritz method [18] is applied to analyze the linear vibrations of the structure. The linear vibrations of the truncated conical shell take the form

$$\begin{bmatrix} u \\ v \\ w \\ \psi_x \\ \psi_y \end{bmatrix} = \begin{bmatrix} U_n(x)\cos(n\varphi) \\ V_n(x)\sin(n\varphi) \\ W_n(x)\cos(n\varphi) \\ X_n(x)\cos(n\varphi) \\ Y_n(x)\sin(n\varphi) \end{bmatrix} \cos(\omega t),$$

where ω is the frequency of the structural vibrations; n is number of circumferential waves. The functions $U_n(x)$, $V_n(x)$, $W_n(x)$, $X_n(x)$, $Y_n(x)$ are presented in the following form

$$U_n(x) = \sum_{i=1}^{N_1} A_i \vartheta_i(x); \quad V_n(x) = \sum_{i=1}^{N_2} A_{N_1+i} \vartheta_i(x); \quad W_n(x) = \sum_{i=1}^{N_3} A_{N_1+N_2+i} \vartheta_i(x);$$

$$X_n(x) = \sum_{i=1}^{N_4} A_{N_1+N_2+N_3+i} \vartheta_i(x); \quad Y_n(x) = \sum_{i=1}^{N_5} A_{N_1+N_2+N_3+N_4+i} \vartheta_i(x), \tag{7}$$

where $N_*=N_1+N_2+N_3+N_4+N_5$; $A=[A_1, \ldots, A_{N*}]$ are unknown parameters, which are obtained from the Rayleigh–Ritz method. The trial functions $\vartheta_i(x)$ take the form $\vartheta_i(x) = \sin\left[\dfrac{(2i-1)\pi(L_2-L_1-x)}{2(L_2-L_1)}\right]$. The expansions (7) are substituted into the kinetic and the potential energies.

$$T_\Sigma = \omega^2 \sin^2(\omega t)\, \widetilde{T}_\Sigma; \quad \Pi_\Sigma = \cos^2(\omega t)\, \widetilde{\Pi}_\Sigma.$$

The least action principle is used as

$$\delta \int_0^{2\pi/\omega} (T_\Sigma - \Pi_\Sigma)\, dt = 0.$$

The following equation is true

$$\int_0^{2\pi/\omega} (T_\Sigma - \Pi_\Sigma)\, dt = \frac{\pi}{\omega}\left[\widetilde{\Pi}_\Sigma(A_1,\ldots,A_{N*}) - \omega^2 \widetilde{T}_\Sigma(A_1,\ldots,A_{N*})\right].$$

The functional stationary value satisfies the equations

$$\frac{\partial}{\partial A_i}\left(\widetilde{\Pi}_\Sigma - \omega^2 \widetilde{T}_\Sigma\right) = 0;\ i=1\ldots N_*.$$

These equations are transformed into the generalized eigenvalue problem

$$[\widetilde{C} - \omega^2 \widetilde{M}]A = 0,$$

where $\widetilde{C}$, $\widetilde{M}$ are stiffness and mass matrixes.

Numerical analysis of vibrations

Parameters of linear vibrations of the cantilever thin-walled structure are analyzed. Mechanical properties of the nanotubes and the matrix are the following:

$\eta_1=0.141$; $\eta_2=1.585$; $\eta_3=1.109$; $E_{11}^{CNT}=2.247\times10^{11}$ Pa; $E_{22}^{CNT}=5.5027\times10^{9}$ Pa; $G_{12}^{CNT}=1.436\times10^{9}$ Pa;

$\mu_{12}^{CNT}=0.2938$; $\mu_{21}^{CNT}=0.007194$; $\rho^{CNT}=1400$ kg/m^3; $\rho^{m}=1150$ kg/m^3; $\mu^{m}=0.34$; $E^{m}=2.5$ GPa.

The conical shell geometrical parameters are the following:

$L_1=0.225$ m; $L_2=0.5$ m; $h=5\times10^{-3}$ m.

The ring is produced from aluminum alloy 518.0 with density $\rho_r=2640$ kg/m3; Young's modulus $E=0.71\times10^{11}$ Pa; Poisson's ratio $\mu=0.33$; shear module $G=2.7\times10^{10}$ Pa. The ring cross section parameters are the following: height $h=10\times10^{-3}$ m and width b=5×10^{-3} m.

The eigenfrequencies and eigenmodes of the vibrations are calculated by the Rayleigh-Ritz method. Uniform nanotube reinforcements are applied for conical shell with V_{CNT}^{*} =0.28. The expansion (7) contains the numbers of terms: N_1=N_2=N_3=N_4=N_5=N. The obtained eigenfrequencies are shown in Table 2. The first twenty-seven eigenfrequencies are given in this table. The first and the second columns of the Table show the eigenfrequencies numbers and the numbers of terms of (25). The third column shows the numbers of circumferential waves n. The fourth column shows the Rayleigh-Ritz eigenfrequencies ω_i in Hz. The fifth column shows the eigenfrequencies $\overline{\omega}_i$ calculated by commercial ANSYS software. The sixth column presents the eigenfrequencies relative differences δ_i.

As the structure vibrations contain two conjugate modes, all eigenfrequencies shown in Table 2 are multiple. Fig. 5 shows the first three eigenmodes, which are obtained by the commercial ANSYS software.

Table 2. Eigenfrequencies of thin-walled structure

N^*	N	n	ω_i, Hz	ANSYS $\overline{\omega}_i$, Hz	δ
1	7	2	669.75	670.74	0.001
2	7	3	719.30	690.92	0.040
3	7	4	813.40	764.83	0.060
4	7	5	892.85	851.41	0.040
5	7	1	900.21	907.69	0.008
6	7	6	988.13	966.06	0.020
7	7	7	1113.21	1113.40	1.7×10^{-4}
8	7	8	1270.38	1290.70	0.015
9	7	2	1456.07	1464.10	0.005
10	7	9	1455.92	1493.50	0.025
11	7	3	1514.83	1522.70	0.005
12	7	10	1665.04	1717.00	0.030
13	7	4	1746.16	1724.10	0.010
14	7	1	1703.22	1736.10	0.019
15	7	5	1920.74	1874.40	0.020
16	7	11	1893.43	1958.10	0.030
17	7	6	2037.56	1995.10	0.020
18	7	7	2151.15	2126.80	0.010
19	7	12	2137.8	2214.60	0.030
20	7	8	2286.92	2286.00	4×10^{-4}
21	7	9	2455.23	2480.90	0.010
22	7	2	2483.21	2481.60	6.48×10^{-4}
23	7	13	2396.87	2486.30	0.035
24	7	3	2531.27	2521.70	0.0037
25	7	1	2606.84	2635.10	0.010
26	7	10	2659.80	2712.20	0.019
27	7	14	2669.31	2772.00	0.037

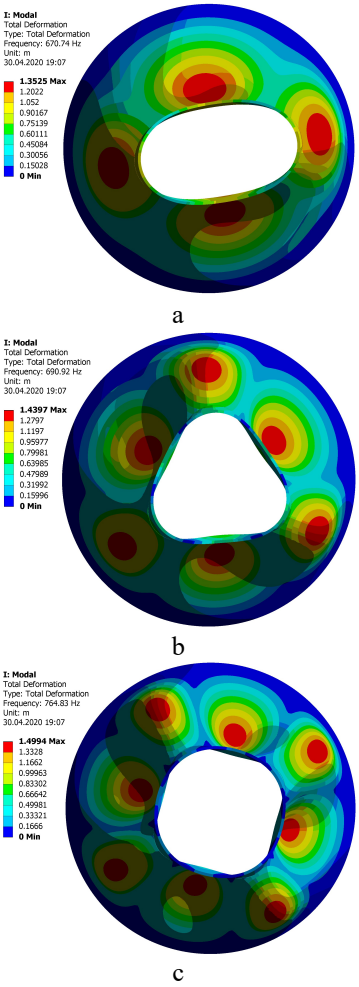

Fig. 5. Eigenmodes corresponding to the eigenfrequencies: a – 670.74 Hz; b – 690.92 Hz; c – 764.83 Hz

Conclusions

The dynamic stressed state of the composite conical shell with nanotube reinforcements is analyzed. Mathematical linear model of this structural vibration is developed using higher order shear theory. In order to obtain the correct mathematical model, the strains are presented up to cubic summands with respect to the lateral coordinate. The potential and kinetic energies are presented up to five order summands with respect to the shell lateral coordinate. The deformation behavior of the isotropic ring is considered in mathematical model of the thin-walled structure. This deformation behavior is described by the Euler-Bernoulli theory. Using the matching of the rotation angles and displacements, all unknowns are transformed to the shell generalized displacements. Thus, the linear mathematical model of thin-walled structural vibrations is derived.

The eigenfrequencies and eigenmodes are analyzed by using the Rayleigh-Ritz method. The results are validated by using the commercial ANSYS software. As follows from the results of numerical analysis, the eigenfrequencies spectrum is very dense.

Acknowledgement

This investigation is particularly supported by grant 0120U101241 from National Academy of Science of Ukraine.

References

1. Gibson, R. F., Ayorinde, E. O., & Wen, Y.-F. (2007). Vibrations of carbon nanotubes and their composites: A review. *Composites Science and Technology*, vol. 67, iss. 1, pp. 1–28. https://doi.org/10.1016/j.compscitech.2006.03.031.
2. Liu, Y. J. & Chen, X. L. (2003). Evaluations of the effective material properties of carbon nanotube-based composites using a nanoscale representative volume element. *Mechanics of Materials*, vol. 35, iss. 1–2, pp. 69–81. https://doi.org/10.1016/S0167-6636(02)00200-4.
3. Odegard, G. M., Gates, T. S., Wise, K. E., Park, C., & Siochi, E. J. (2003). Constitutive modeling of nanotube–reinforced polymer composites. *Composites Science and Technology*, vol. 63, iss. 11, pp. 1671–1687. https://doi.org/10.1016/S0266-3538(03)00063-0.
4. Allaoui, A., Bai, S., Cheng, H. M., & Bai, J. B. (2002). Mechanical and electrical properties of a MWNT/epoxy composite. *Composites Science and Technology*, vol. 62, iss. 15, pp. 1993–1998. https://doi.org/10.1016/S0266-3538(02)00129-X.
5. Ci, L. & Bai, J. (2006). The reinforcement role of carbon nanotubes in epoxy composites with different matrix stiffness. *Composites Science and Technology*, vol. 66, iss. 3–4, pp. 599–603. https://doi.org/10.1016/j.compscitech.2005.05.020.
6. Richard, P., Prasse, T., Cavaille, J. Y., Chazeau, L., Gauthier, C., & Duchet, J. (2003). Reinforcement of rubbery epoxy by carbon nanofibres. *Materials Science and Engineering: A*, vol. 352, iss. 1–2, pp. 344–348. https://doi.org/10.1016/S0921-5093(02)00895-X.
7. Nejati, M., Asanjarani, A., Dimitri, R., & Tornabene, F. (2017). Static and free vibration analysis of functionally graded conical shells reinforced by carbon nanotubes. *International Journal of Mechanical Sciences*, vol. 130, pp. 383–398. https://doi.org/10.1016/j.ijmecsci.2017.06.024.
8. Jafari Mehrabadi, S. & Sobhani, A. B. (2014). Stress analysis of functionally graded open cylindrical shell reinforced by agglomerated carbon nanotubes. *Thin-Walled Structures*, vol. 80, pp. 130–141. https://doi.org/10.1016/j.tws.2014.02.016.
9. Zhang, L. W., Lei, Z. X., Liew, K. M., & Yu, J. L. (2014). Static and dynamic of carbon nanotube reinforced functionally graded cylindrical panels. *Composite Structures*, vol. 111, pp. 205–212. https://doi.org/10.1016/j.compstruct.2013.12.035.
10. García-Macías, E., Rodríguez-Tembleque, L., & Sáez A. (2018). Bending and free vibration analysis of functionally graded graphene vs. carbon nanotube reinforced composite plates. *Composite Structures*, vol. 186, pp. 123–138. https://doi.org/10.1016/j.compstruct.2017.11.076.
11. Lei, Z. X., Liew, K. M., & Yu J. L. (2013). Free vibration analysis of functionally graded carbon nanotube-reinforced composite plates using the element-free kp-Ritz method in thermal environment. *Composite Structures*, vol. 106, pp. 128–138. https://doi.org/10.1016/j.compstruct.2013.06.003.
12. Lei, Z. X., Zhang, L. W., & Liew, K. M. (2015). Elastodynamic analysis of carbon nanotube-reinforced functionally graded plates. *International Journal of Mechanical Sciences*, vol. 99, pp. 208–217. https://doi.org/10.1016/j.ijmecsci.2015.05.014.
13. Moradi-Dastjerdi, R., Foroutan, M., & Pourasghar, A. (2013). Dynamic analysis of functionally graded nanocomposite cylinders reinforced by carbon nanotube by a mesh-free method. *Materials & Design*, vol. 44, pp. 256–266. https://doi.org/10.1016/j.matdes.2012.07.069.
14. Reddy, J. N. (1984). A refined nonlinear theory of plates with transverse shear deformation. *International Journal of Solids and Structures*, vol. 20, iss. 9–10, pp. 881–896. https://doi.org/10.1016/0020-7683(84)90056-8.
15. Amabili, M. & Reddy, J. N. (2010). A new non-linear higher-order shear deformation theory for large-amplitude vibrations of laminated doubly curved shells. *International Journal of Non-Linear Mechanics*, vol. 45, iss. 4, pp. 409–418. https://doi.org/10.1016/j.ijnonlinmec.2009.12.013.
16. Vlasov, V. Z. (1961). Thin-Walled Elastic Beams. Jerusalem: Israel Program for Scientific Translations, 493 p.
17. Amiro, I. Ya. & Zarutskiy, V. A. (1980). *Metody rascheta obolochek* [Methods of shells calculations]. Vol. 2. *Teoriya rebristykh obolochek* [Theory of ribbed shells]. Kyiv: Naukova Dumka, 368 p. (in Russian).
18. Meirovitch, L. (1986). Elements of Vibration Analysis. New York: McGraw-Hill Publishing Company.

Received 02 February 2026 *Accepted 03 March 2026* *Published 30 March 2026*

Лінійні коливання композитної конічної оболонки, армованої нанотрубками, з кільцевим елементом жорсткості

[1] К. В. Аврамов, [1] Б. В. Успенський, [2] Б. Г. Любарський, [2] О. А. Смецьких, [1] І. В. Біблік

[1] Інститут енергетичних машин і систем ім. А. М. Підгорного НАН України,
61046, Україна, м. Харків, вул. Комунальників, 2/10

[2] Національний технічний університет «Харківський політехнічний інститут»,
61002, Україна, м. Харків, вул. Кирпичова, 2

Досліджуються лінійні коливання тонкостінної конструкції, що складається з конічної оболонки, армованої нанотрубками, і кільця, що посилює конструкцію. Армування нанотрубками проводиться так, що матеріал конічної оболонки є функціонально-градієнтним. Кільце кріпиться на кінці усіченої конічної оболонки. Така конструкція є моделлю адаптера ракетоносія. Доводиться, що для ракетобудування актуальним завданням виступає динаміка даної конструкції. Матеріал оболонки є нанокомпозитом, а кільце виготовлено з ізотропного матеріалу. Для моделювання напруженого стану оболонки використовується теорія зсуву високого порядку та теорія Ейлер-Бернулі для моделювання кільця. Передбачається, що кільце здійснює згинальні коливання у двох площинах, окружні переміщення і крутильні коливання. Для виведення рівнянь коливань конструкції застосовується метод Релея-Рітца. Після цього використовується потенційна енергія тонкостінної конструкції, яка складається з потенційної енергії конічної оболонки і потенційної енергії кільця. Завдяки варіаційному принципу Остроградського-Гамільтона приходимо до узагальненої проблеми власних значень. Результати розрахунку власних частот верифікуються кінцево-елементними розрахунками у програмному комплексі ANSYS.

***Ключові слова**: функціонально-градієнтний композит, армований вуглецевими нанотрубками, усічена конічна оболонка, параметри лінійних коливань.*

Література

1. Gibson R. F., Ayorinde E. O., Wen Y.-F. Vibrations of carbon nanotubes and their composites: A review. *Composites Science and Technology*. 2007. Vol. 67. Iss. 1. P. 1–28. https://doi.org/10.1016/j.compscitech.2006.03.031.
2. Liu Y. J., Chen X. L. Evaluations of the effective material properties of carbon nanotube-based composites using a nanoscale representative volume element. *Mechanics of Materials*. 2003. Vol. 35. Iss. 1–2. P. 69–81. https://doi.org/10.1016/S0167-6636(02)00200-4.
3. Odegard G. M., Gates T. S., Wise K. E., Park C., Siochi E. J. Constitutive modeling of nanotube–reinforced polymer composites. *Composites Science and Technology*. 2003. Vol. 63. Iss. 11. P. 1671–1687. https://doi.org/10.1016/S0266-3538(03)00063-0.
4. Allaoui A., Bai S., Cheng H. M., Bai J. B. Mechanical and electrical properties of a MWNT/epoxy composite. *Composites Science and Technology*. 2002. Vol. 62. Iss. 15. P. 1993–1998. https://doi.org/10.1016/S0266-3538(02)00129-X.
5. Ci L., Bai J. The reinforcement role of carbon nanotubes in epoxy composites with different matrix stiffness. *Composites Science and Technology*. 2006. Vol. 66. Iss. 3–4. P. 599–603. https://doi.org/10.1016/j.compscitech.2005.05.020.
6. Richard P., Prasse T., Cavaille J. Y., Chazeau L., Gauthier C., Duchet J. Reinforcement of rubbery epoxy by carbon nanofibres. *Materials Science and Engineering: A*. 2003. Vol. 352. Iss. 1–2. P. 344–348. https://doi.org/10.1016/S0921-5093(02)00895-X.
7. Nejati M., Asanjarani A., Dimitri R., Tornabene F. Static and free vibration analysis of functionally graded conical shells reinforced by carbon nanotubes. *International Journal of Mechanical Sciences*. 2017. Vol. 130. P. 383–398. https://doi.org/10.1016/j.ijmecsci.2017.06.024.
8. Jafari Mehrabadi S., Sobhani A. B. Stress analysis of functionally graded open cylindrical shell reinforced by agglomerated carbon nanotubes. *Thin-Walled Structures*. 2014. Vol. 80. P. 130–141. https://doi.org/10.1016/j.tws.2014.02.016.
9. Zhang L. W., Lei Z. X., Liew K. M., Yu J. L. Static and dynamic of carbon nanotube reinforced functionally graded cylindrical panels. *Composite Structures*. 2014.Vol. 111. P. 205–212. https://doi.org/10.1016/j.compstruct.2013.12.035.
10. García-Macías E., Rodríguez-Tembleque L., Sáez A. Bending and free vibration analysis of functionally graded graphene vs. carbon nanotube reinforced composite plates. *Composite Structures*. 2018. Vol. 186. P. 123–138. https://doi.org/10.1016/j.compstruct.2017.11.076.
11. Lei Z. X., Liew K. M., Yu J. L. Free vibration analysis of functionally graded carbon nanotube-reinforced composite plates using the element-free kp-Ritz method in thermal environment. *Composite Structures*. 2013.Vol. 106. P. 128–138. https://doi.org/10.1016/j.compstruct.2013.06.003.

12. Lei Z. X., Zhang L. W., Liew K. M. Elastodynamic analysis of carbon nanotube-reinforced functionally graded plates. *International Journal of Mechanical Sciences*. 2015. Vol. 99. P. 208–217. https://doi.org/10.1016/j.ijmecsci.2015.05.014.
13. Moradi-Dastjerdi R., Foroutan M., Pourasghar A. Dynamic analysis of functionally graded nanocomposite cylinders reinforced by carbon nanotube by a mesh-free method. *Materials & Design*. 2013. Vol. 44. P. 256–266. https://doi.org/10.1016/j.matdes.2012.07.069.
14. Reddy J. N. A refined nonlinear theory of plates with transverse shear deformation. *International Journal of Solids and Structures*. 1984. Vol. 20. Iss. 9–10. P. 881–896. https://doi.org/10.1016/0020-7683(84)90056-8.
15. Amabili M., Reddy J. N. A new non-linear higher-order shear deformation theory for large-amplitude vibrations of laminated doubly curved shells. *International Journal of Non-Linear Mechanics*. 2010. Vol. 45. Iss. 4. P. 409–418. https://doi.org/10.1016/j.ijnonlinmec.2009.12.013.
16. Vlasov V. Z. Thin-Walled Elastic Beams. Jerusalem: Israel Program for Scientific Translations, 1961. 493 p.
17. Амиро И. Я., Заруцкий В. А. Методы расчета оболочек. Т. 2. Теория ребристых оболочек. Киев: Наукова думка, 368 с.
18. Meirovitch L. Elements of Vibration Analysis. New York: McGraw-Hill Publishing Company, 1986.